

International Journal of Thermophysics

Measuring humidity in methane and natural gas with a microwave technique

--Manuscript Draft--

Manuscript Number:	
Full Title:	Measuring humidity in methane and natural gas with a microwave technique
Article Type:	TEMPMEKO 2013 Special Issues
Keywords:	microwave hygrometry; natural gas
Corresponding Author:	Roberto Maria Gavioso, Ph. D. INRIM Torino, ITALY
Corresponding Author Secondary Information:	
Corresponding Author's Institution:	INRIM
Corresponding Author's Secondary Institution:	
First Author:	Roberto Maria Gavioso, Ph. D.
First Author Secondary Information:	
Order of Authors:	Roberto Maria Gavioso, Ph. D. Daniele Madonna Ripa Robert Benyon Jaime Garcia Gallegos Fernando Perez-Sanz Simone Corbellini Susana Avila Angel Maria Benito
Order of Authors Secondary Information:	
Abstract:	<p>We report the results of microwave measurements with a quasi-spherical resonator in humid methane samples realized under laboratory conditions at INRiM and under industrial conditions in a natural gas sample made available at the facilities of ENAGAS (Technical Manager of the Spanish Gas System and main supplier of natural gas in Spain). Measurements at INRiM included vapor phase and condensation tests on methane samples prepared with volume water fractions between 600 ppm and 5000 ppm at temperatures between 273 K and 295 K and pressures between 150 kPa and 1 MPa. ENAGAS measurements were performed at ambient temperature, 750 kPa on natural gas sampled from the pipeline and successively humidified at volume water fractions between 140 ppm and 250 ppm for completeness of the comparison with several humidity sensors and instrumentation based on different technologies. To enhance the sensitivity of the microwave method at low humidity, we conceived and implemented an experimental procedure based on the relative comparison of the dielectric permittivity of the humid gas sample before and after being subject to a chemical drying process. The uncertainty budget and the final sensitivity of this procedure is discussed.</p>
Suggested Reviewers:	Stephanie Bell NPL Stephanie.Bell@npl.co.uk expert in this field

Measuring humidity in methane and natural gas with a microwave technique

1
2
3
4
5
6
7
8
9
10
11
12
13
14
15
16
17
18
19
20
21
22
23
24
25
26
27
28
29
30
31
32
33
34
35
36
37
38
39
40
41
42
43
44
45
46
47
48
49
50
51
52
53
54
55
56
57
58
59
60
61
62
63
64
65

R. M. Gavioso^{1,6}, D. Madonna Ripa¹, R. Benyon², J. G. Gallegos², F. Perez-Sanz³, S. Corbellini⁴, S. Avila⁵ and A. M. Benito⁵

¹ Thermodynamics Division, Istituto Nazionale di Ricerca Metrologica, Torino, Strada delle Cacce 91
10135, Italy

² Instituto Nacional de Técnica Aeroespacial, Torrejón de Ardoz, Spain

³ Universidad de Valladolid, Valladolid, Spain

⁴ Politecnico di Torino, Torino, Italy

⁵ ENAGAS, SA, Zaragoza, Spain

⁶ To whom correspondence should be addressed. E-mail: r.gavioso@inrim.it

Abstract

1
2 We report the results of microwave measurements with a quasi-spherical resonator in humid methane
3
4 samples realized under laboratory conditions at INRiM and under industrial conditions in a natural gas
5
6 sample made available at the facilities of ENAGAS (Technical Manager of the Spanish Gas System and
7
8 main supplier of natural gas in Spain). Measurements at INRiM included vapor phase and condensation tests
9
10 on methane samples prepared with volume water fractions between 600 ppm and 5000 ppm at temperatures
11
12 between 273 K and 295 K and pressures between 150 kPa and 1 MPa. ENAGAS measurements were
13
14 performed at ambient temperature, 750 kPa on natural gas sampled from the pipeline and successively
15
16 humidified at volume water fractions between 140 ppm and 250 ppm for completeness of the comparison
17
18 with several humidity sensors and instrumentation based on different technologies. To enhance the
19
20 sensitivity of the microwave method at low humidity, we conceived and implemented an experimental
21
22 procedure based on the relative comparison of the dielectric permittivity of the humid gas sample before and
23
24 after being subject to a chemical drying process. The uncertainty budget and the final sensitivity of this
25
26 procedure is discussed.
27
28
29
30

31 **In alphabetical order:**

32
33 **Keywords:** Microwave hygrometry; Natural gas
34
35
36
37
38
39
40
41
42
43
44
45
46
47
48
49
50
51
52
53
54
55
56
57
58
59
60
61
62
63
64
65

1 Introduction

In response to broad social and economic triggers and particular industrial needs [1], new standards and measurement methods for humidity are being developed in metrological laboratories with the objective of extending their covered temperature and pressure range and the capability to traceably prepare and measure the water content of a variety of non-air gases.

Within this framework of activities, improving the characterization of humidity in natural gas would reduce the cost and the environmental impact of its industrial heat treatment prior to supply to a delivery grid. The ideal instrument to accomplish this task would be robust, to sustain typical pipeline conditions (up to 7 MPa) possibly during the course of the glycol dehydrating process, and would provide an estimate of the water volume fraction x_w over the range of interest for natural gas applications (10 ppm to 300 ppm) with a relative uncertainty in the order of a few ppm and being insensitive to moderate variations of the composition of the dry fraction of the mixture. However, the current practice for these measurements is mostly limited to sampling downstream the dehydration process with instruments which either estimate x_w relying on the results of a previous calibration at rather different conditions (e.g. in nitrogen at ambient temperature and pressure) or imply a determination of the dew- or frost-point temperature of the humid mixture with an accuracy which is impaired by the uncertainty associated to the enhancement factor. Additionally, condensation type hygrometers have to deal with the difficulty of discriminating between the separate or contemporary multiphase condensation of hydrocarbons and water.

Previous applications of microwave resonators to the determination of the electrical [2] and thermophysical properties of hydrocarbon mixtures, including cricondenterms [3], was demonstrated using a re-entrant cavity [4]. Later, accurate humidity measurements were achieved using a quasi-spherical microwave resonator (QSR) with humid air and nitrogen mixtures over a limited pressure and temperature range [5, 6].

In this work, we report the results of preliminary tests and the on-site application of a QSR to discuss its potential usefulness in the context of hydrocarbons and natural gas hygrometry. This is favored by the ruggedness of the resonator and by its two-fold operation method, which can either determine x_w from measurements in vapor phase, or alternatively determine the dew- or frost-point temperature working in saturation conditions. In view of field application, the preparatory work conducted at INRiM, including both vapor phase and condensation tests with humid methane mixtures between 273 K and 300 K for pressures up to 1 MPa, highlighted the criticality achieving useful accuracy for vapor phase measurements for mixtures having x_w below 1000 ppm, as a consequence the relevant uncertainty contribution in the determination of the mixture density. To mitigate this difficulty, an original measurement procedure was conceived which implies the consecutive flow through the microwave cavity of the humid mixture and of its

dry fraction. Upon realization of a suitable chemical drying manifold, this procedure was implemented for a few on-site tests with a natural gas sample and compared to the response of several commercial or prototype instruments including several capacitive metal oxide sorbative sensors (Al_2O_3 , P_2O_5), as well as a diode laser absorption spectrometer and polymer sensors, on a dedicated experimental rig [7]. Due to the extreme dryness revealed by the natural gas sample under test, initially estimated from laser absorption spectroscopy measurement during the installation of the test rig of $x_w \sim 4$ ppm, and to enhance the meaningfulness of the comparison, the sample was humidified using a custom divided flow generator, increasing x_w to the range between 50 ppm and 200 ppm. Remarkably, the microwave method traced the changes in the humidity of the sample and its determination of x_w was found to be consistent within the wide ranging different readings of the commercial instruments.

In Section 2, we summarize preliminary tests and results conducted at INRiM with humid methane mixtures, including the determination of the enhancement factor of humid methane near 273.15 K at absolute pressures 150 kPa and 750 kPa. The overall outcome of these tests and their uncertainty analysis indicated that the accuracy of a determination of x_w with a standard measurement procedure is severely limited for x_w below 1000 ppm, reducing the applicability of the method; In Section 3, we discuss the basic principles of an alternative measurement procedure conceived to overcome the previous difficulties by the alternative flow through the microwave cavity of the humid sample under test as is, or upon being subject to flow through a drying manifold. Section 4 describes the practical implementation of this measurement procedure for on-site tests at ENAGAS, which included the first practical test of dedicated electronics for the acquisition of microwave frequency data, in replacement of the otherwise costly and bulky network analysis instrumentation. Also, within the same section we discuss the results obtained during the limited slot available for the tests at ENAGAS using the QSR, prior to the full comparison of industrial instruments reported in [7]. Finally, the concluding section briefly discusses the perspectives of improvement and the future developments of the proposed microwave method.

2 Preliminary laboratory measurements with humid methane mixtures

2.1 Experimental setup

The QSR used in this work is a gold-plated maraging steel triaxial ellipsoid, with a nominal average radius $a = 2.54$ cm, previously used for humidity measurements in air and nitrogen at INRiM and NPL, whose performance and detailed description is given elsewhere [5, 6]. Minor modifications to the electrical and mechanical configuration of the resonator were brought in preparation for the measurements described here, including the realization and test of new microwave loop probes, mount of a couple of recently calibrated

platinum resistance thermometers (PRTs) and modification of the mechanical support of the QSR and its hydraulic connections to match the features and dimensions of the thermostat and the pressure vessel available at INRiM. Figure 1 illustrates the basic components and features of the flow-pressure-temperature control and gas-handling systems. Coarse temperature control of the QSR was maintained by flowing liquid ethanol from an external circulating thermostat. The finer PID temperature control needed for a precise determination of dew points during condensation tests was provided by a low power electrical heater in contact with the inlet connection to the thermostat. The temperature of the gas was estimated from the readings of two capsule PRTs, embedded in copper plates in contact with the lower and upper parts of the resonator shell. Unfortunately, in spite of a satisfactory stability performance of the thermostating system, the difference in the readings of the two PRTs, previously calibrated against a secondary standard with an expanded uncertainty of 0.01 K, was found to increase from a minimum of few mK up to as much as 0.15 K as a function of the temperature, limiting the accuracy of the estimate of the gas temperature within the QSR. A mass-flow control on the inlet flow to the QSR and PID electro-actuated valve on the outlet vent maintained the pressure stable within ± 10 Pa of the selected pressure set-point, based on the readings of a capacitive pressure transducer with a full-scale range of 20000 Torr, at variable flow rates between 5 and 500 sccm. The manifold sketched in Fig. 1 could be employed to prepare a humid methane mixture by flowing 0.99995 % pure methane from a high-pressure sampling bottle through a simple humidity generator in the form of a pressure-tight bubbler, or alternatively, by direct sampling from a purchased mixture with a nominal concentration of 1000 ppm of water in methane at a maximum pressure of 250 kPa. In the former scheme, the water in the bubbler had been prepared by extended pumping at a few hPa of a filtered, deionized sample and repeated freeze-pump-thaw cycles to remove any significant amount of dissolved gases above and within the liquid. Initially, the saturator was inserted within a refrigerated container to have the possibility to vary its temperature. However, the measured variations of the humidity of the generated mixture were later found to be excessively large, and for subsequent tests it was decided to improve the thermostating of the saturator by placing it inside a vacuum insulated dewar filled with a water/ice bath.

2.2 Preliminary measurements in vacuum, nitrogen and methane

Working away from saturation, the permittivity ε_r of a pure gas or a gaseous mixture is determined from the squared ratio

$$\varepsilon_r = \frac{1}{\mu_r} \left(\frac{\langle f_{ln}^\sigma + g_{ln}^\sigma \rangle_0}{\langle f_{ln}^\sigma + g_{ln}^\sigma \rangle_p (1 - k_T p/3)} \right)^2 \quad (1)$$

where $\langle f \rangle$ and $\langle g \rangle$ are respectively the average frequency and average halfwidth a triply-degenerate (with single components identified by the set of indexes l, n, σ) microwave mode of a QSR cavity measured at the same temperature T both in vacuum (subscript 0) and at pressure p . In Eq. 1 it is usually a good approximation to assume the magnetic permeability of the gas $\mu_r = 1$ (with the notable exception of oxygen) while the isothermal compressibility k_T of the metal comprising the resonator, which accounts for pressure induced changes of the cavity dimensions, can be determined from measurements as a function of pressure with helium gas.

An interpolation of the vacuum frequencies as a function of temperature leads to a precise empirical determination of the thermal expansion coefficient α_{th} of the resonator, which is then routinely used to account for the variation of the cavity dimension with temperature. In the preparatory phase of this work, the vacuum frequencies of the four lowest frequency modes TM11 to TE12 were measured between 250 K and 300 K and fitted to a quadratic expansion $\langle f_{ln}^\sigma \rangle_0(T) = \langle f_{ln}^\sigma \rangle_0^{T_{ref}} - \alpha_{th}(T - T_{ref}) - \beta_{th}(T - T_{ref})^2$ with $T_{ref} = 273.15$ K and the leading coefficient $\alpha_{th} = (9.71 \pm 0.02) \text{ K}^{-1}$, in good agreement with tabulated values for maraging steel.

As an initial test of the overall performance of the apparatus, the frequencies of the four triplets TM11 to TE12 were measured while nitrogen, and successively methane were flowing through the QSR at a rate of 50 sccm, at pressures in the range between 150 kPa and 1.5 MPa at 293.15 K. From these data, we determined the permittivity of pure N_2 and CH_4 using Eq. (1) and compared it to the expected value of the same quantities as calculated from their thermodynamic and electrical properties [8, 9, 10]. Figure 2 illustrates the fractional deviations of these comparisons. There, it is evident that the quality of the agreement is only partially satisfactory for both gases, with relative deviations tracing hysteretic trends which correlated with the sign of the pressure variations during the experimental runs. As a plausible justification of these trends, we remark that the capacitive pressure transducer, which was not calibrated against a primary standard prior to these measurements, has a previous historical calibration record which showed similar hysteretic behavior, with typical deviations from the standard of ± 200 Pa. Thus, it is likely that hysteresis in these trends results from an imperfect laboratory realization of the pressure. Additionally, with respect to nitrogen data, methane data show a negative mean deviation from the baseline of about -5 ppm, suggesting the presence of impurities in the test gas. The consequences of these inconsistencies and their contribution to the uncertainty of a determination of the composition of methane/water mixtures is discussed below in Section 3.

2.3 Vapor phase measurements in humid methane

Using the apparatus sketched in Fig. 1, humid methane mixtures were prepared initially by flowing dry methane through a basic humidity generator in the form of a bubbler. The temperature of the generator was kept approximately constant at about $(4.0 \pm 0.5)^\circ\text{C}$ within a refrigerated container while the temperature of the QSR was maintained near 20°C by the liquid bath thermostat. The absolute pressure within the saturator and the QSR was first increased between 150 kPa and 1 MPa, and successively decreased back to its initial value. At each pressure, microwave data for four modes TM11 to TE12 were recorded for approximately one hour. From the recorded data, assuming that the mixture contains only methane and water vapor, and using independent estimates of the virial coefficients and the permittivities of these substances, we calculated the water mole fraction x_w of the generated mixture as a function of pressure using the procedure described in Eqs. 1-4 of Ref. 5. Particularly, to use this method with a mixture of methane and water, the second virial coefficient of water B_w was taken from [11], the second virial coefficient of methane from [9] the cross-second virial coefficient B_{wd} of the methane-water system from [12]. Finally, the dielectric constant of water vapor as a function of temperature was taken from [13] and that of methane from [14]. From the results of this estimate of x_w (Fig. 3), it is evident that the poor temperature stability of the saturator impaired its capability to generate a mixture with a stable concentration of water vapor (see the sinusoidally oscillating variation of x_w as a function of time in Fig. 3, which is particularly evident at low pressure). To improve thermal stability the generator was later inserted in a dewar in contact with a melting water-ice mixture. With this arrangement the temperature of the bubbler stayed approximately constant and slightly above 273.15 K for several days. The data on the left side of Fig. 3 clearly show the change of solubility of water in compressed CH_4 over the range 150 kPa to 1 MPa, which approximately agree (blue curve in Fig. 3) with the limiting value $x_{\text{eq}} = e_w(T_{\text{sat}})/p$, where $e_w(T)$ is the saturation vapor pressure of pure water, $T_{\text{sat}} \approx 4^\circ\text{C}$ and p is the total pressure. This limit should be attained when thermodynamic equilibrium is onset in the saturator between the condensed liquid phase and the gaseous mixture. As pressure is further increased away from ideality, the following modification to this simple rule holds:

$$x_{\text{eq}} = \frac{e_w(T)}{p} \exp[\Phi(p, T)] \quad (2)$$

where $\Phi(p, T)$ is some function of the virial coefficients of the mixture and the molar volume of both water vapor and liquid water [15]. At any fixed temperature, high pressure conditions (corresponding to increasingly lower water molar fractions and highly dilute mixtures) do evidence the effect of unlike molecular interactions, causing the saturated vapor pressure of water to deviate from its pure substance value $e_w(T)$. The relative amount of such deviation $f(p, T)$ is a function of temperature and total pressure and

takes the name of enhancement factor. We remark that the pressure range explored in this initial test (max. 1 MPa) is still so moderately away from ideality that it should not surprise that this deviation is not visually evident on the scale of the graph in Fig. 3.

2.4 Condensation tests and determination of the enhancement factor of humid methane

Away from saturation, the ratio of any two mode eigenvalues of the microwave cavity is expected to be a stable property of the cavity geometrical shape which is independent of the gas composition and density. Also, if the thermal expansion and the elastic deformation of the cavity under hydrostatic pressure are isotropic these ratios are expected to remain constant even when the temperature of the resonator and the hydrostatic pressure are varied. This property was indeed well verified for the ratio TM11/TE11 for all the fluids and measurement conditions illustrated above (see data in Table I and Fig. 4), confirming it to be an extremely stable and repeatable reference.

To determine the dew-point temperature T_{dp} of a humid mixture, the experimental procedure consists in decreasing the temperature of the QSR until a decrease of the otherwise constant TM11/TE11 mode ratio is detected, revealing the onset of a condensate layer on the internal surface of the resonator [6]. When this condition is met, the temperature of the resonator is controlled at T_{dp} to maintain equilibrium between evaporation and condensation of the surface layer and the magnitude of the deviation of the TM11/TE11 ratio from its reference value is proportional to the thickness of the condensate.

In this work, the resonator temperature was controlled by fine PID regulation of the power delivered by an electrical heater to the adduction tube flowing the thermostating liquid from the bath to the resonator. As an example of the quality achievable by this control, Fig. 5 displays the final tuning phases of the PID control during condensation tests at 150 kPa and 750 kPa, while humid methane mixtures prepared by the generator at 273.15 K are flown through the QSR at a rate of 50 sccm and 300 sccm respectively.

The data recorded during these condensation tests may be used to determine the enhancement factor of the methane/water mixture from the relation

$$f(p, T_{dew}) = x_w p / e_w(T_{dp}) , \quad (3)$$

where: p is the experimental (total) pressure; T_{dp} is the temperature which stabilizes the difference between the measured TM11/TE11 ratio and its reference value away from condensation; the molar water fraction x_w is calculated from the microwave data recorded for the TE11 mode; $e_w(T_{dp})$ is the saturated vapor pressure of water at T_{dp} , calculated from the IAPWS95 formulation [11]. Figure 7 shows two determinations of $f(p, T)$ near 273 K at 150 kPa ($x_w \approx 4000$ ppm) and 750 kPa ($x_w \approx 800$ ppm), respectively equal to $f(150 \text{ kPa}, 273.25 \text{ K}) = 0.97 \pm 0.09$ and $f(750 \text{ kPa}, 273.30 \text{ K}) = 0.90 \pm 0.15$. (Unless otherwise stated,

all reported uncertainties are standard uncertainties with a coverage factor $k = 1$). We compare these results with previously published estimates of the enhancement factor of the methane/water system in Fig. 7, which was prepared by adapting correlations of the water content of natural gas [16-18]. This comparison shows that the mean values and the uncertainty of our determinations of the enhancement factor of humid methane are barely consistent when compared to the pressure trend of available literature sources and their overall dispersion. The most relevant contributions to the reported uncertainties, and the discussion of an alternative experimental procedure aiming at their reduction are described and discussed hereafter.

3 Uncertainty of a microwave determination of x_w and $f(p, T)$

In the context of hygrometric applications of microwave resonators, the contribution of the uncertainty associated to frequency measurements can be usually kept so small to be negligible with respect to other sources. Among the latter, the uncertainty contribution due to the imperfect estimate of x_w is usually predominant. As an example, at 273.3 K and 750 kPa the temperature uncertainty $u(T) = 0.1$ K contributes by as much as 4×10^{-2} to the relative uncertainty of the numerator in Eq. (3), i.e. the partial pressure of water vapor in the mixture, while it contributes only 6×10^{-3} to the relative uncertainty of the denominator of Eq. 3, i.e. the saturated water pressure. While the overall uncertainty of T_{dp} is mainly determined by temperature errors, the overall uncertainty of x_w has significant contributions from several other sources, including: the imperfect determination of pressure; the validity of the assumptions on composition of the mixture, due to the possible presence of unknown or variable amounts of impurities; the uncertainty contributed by the imperfect knowledge of the thermodynamic properties (virial coefficients) and the electrical properties (polarizability) of the mixture components, which is usually dominated by the uncertainty associated to the Debye constants of water vapor [13]. Thus, the uncertainties for the enhancement factors reported in the previous section and plotted in Fig. 7, were evaluated considering the contributions arising from three main sources: i) our imperfect determination of pressure with a relative standard uncertainty $u_r(p) = 0.05$ % roughly estimated from the typical deviations of the pressure transducer from a reference standard; ii) temperature uncertainty, with a dominant contribution $u(T) = 0.10$ K from the temperature gradient observed between the readings of two thermometer at different locations on the QSR; iii) the uncertainty of the permittivity of dry methane, estimated by the systematic deviation between the results of the preliminary measurements described in § 2.2 (Fig. 2) and literature references to the same quantity [9]. These deviations could in principle allow us to calculate ad-hoc corrections to our experimental data. However, the large temperature difference between our measurements in dry methane and humid methane, and the rather large hysteresis of dry methane data (Fig. 2) discourage from implementing such a correction procedure.

For a humid methane mixture at 293 K, 100 kPa, the red curve in Fig. 8 displays the overall relative uncertainty $u_r(x_w)$ of a determination of the water fraction, considering typical contributions of imperfect pressure $u_r(p) = 0.1\%$ and temperature measurements $u(T) = 0.01$ K and the uncertainty associated with the reference functions or correlations used to predict the thermodynamic and electrical properties of methane and water. The diverging increase of $u_r(x_w)$ for low water fractions is evident, growing approximately as $(x_w)^{-1}$ from 20 % for $x_w \approx 500$ ppm ($T_{dp} \approx 246$ K) to 100 % for $x_w \approx 100$ ppm ($T_{dp} \approx 231$ K). For increasing humidity, $u_r(x_w)$ is ultimately limited at about 1.4 % by the uncertainty of the polarizability of water [11].

Speculating about a possible mitigation of this unfavorable scheme, we remark that the extremely accurate determinations of pressure and temperature which are needed to determine x_w when this quantity is low (i. e. in the majority of cases of interest for the determination of the enhancement factor) are costly and unpractical, prohibiting their use in field measurements and increasing the effort in laboratory determinations. Also, assessing the composition of the dry fraction of the mixture may require considerable effort.

Hereafter we describe an alternative experimental procedure which may significantly reduce these practical difficulties and the uncertainty budget. The procedure is based on a dual measurement of the frequencies of the same microwave cavity when this is alternatively filled with a humid mixture f_{mix} or with its dry fraction f_{dry} . In the laboratory this procedure may be readily achieved if, as it is usual, the dry fraction is available prior to being humidified by a generator. In the field, the dry fraction can be prepared by flowing the humid mixture through a suitable dryer (a cryotrap, or drying cartridges filled with anhydrous chemicals). The configuration of the gas-handling manifold is such that the humid or dry test gases may be alternatively flown through the resonator. During the time needed to the acquisition of both frequency measurements the resonator is maintained at approximately the same pressure and temperature, where it is no longer required that the measurement of p and T would be extremely accurate but only they would be precise and repeatable. For the procedure discussed above, we consider new working equations for the determination of x_w .

The permittivity of the mixture is obtained as:

$$\varepsilon_{\text{mix}}(p, T) = \varepsilon_{\text{dry}}(p, T) \left(\frac{f_{\text{dry}}(p, T)}{f_{\text{mix}}(p, T)} \right)^2. \quad (4)$$

The humid and dry fractions of the mixture respectively have densities ρ_{mix} and ρ_{dry} and polarizabilities:

$$\beta_{\text{mix}} = \frac{1}{\rho_{\text{mix}}} \frac{\varepsilon_{\text{mix}} - 1}{\varepsilon_{\text{mix}} + 2} \quad \text{and} \quad \beta_{\text{dry}} = \frac{1}{\rho_{\text{dry}}} \frac{\varepsilon_{\text{dry}} - 1}{\varepsilon_{\text{dry}} + 2}. \quad (5)$$

We next consider the ratio of the polarizabilities

$$\rho_{\text{mix}} / \rho_{\text{dry}} = \frac{\rho_{\text{dry}}}{\rho_{\text{mix}}} \left(\frac{\epsilon_{\text{mix}} - 1}{\epsilon_{\text{mix}} + 2} \frac{\epsilon_{\text{dry}} + 2}{\epsilon_{\text{dry}} - 1} \right), \quad (6)$$

and, for the sake of simplifying the equations below, we note that when $x_w \ll 1$ it is safe to assume that $\rho_{\text{dry}} = \rho_{\text{mix}}$. As an example of the validity of this assumption, for the fraction $x_w = 1000$ ppm of water in methane at 150 kPa and 275 K, the quantity $\rho_{\text{dry}} / \rho_{\text{mix}}$ differs from unity by only 0.4 ppm. Thus, recalling that $\rho_{\text{mix}} = x_w \rho_w + (1 - x_w) \rho_{\text{dry}}$, we have:

$$x_w = \frac{\left(\frac{\epsilon_{\text{mix}} - 1}{\epsilon_{\text{mix}} + 2} \frac{\epsilon_{\text{dry}} + 2}{\epsilon_{\text{dry}} - 1} \right) - 1}{\rho_w / \rho_{\text{dry}} - 1}. \quad (7)$$

The robustness of Eq. (7) against systematic errors in both the determination of the pressure and the estimate of ϵ_{dry} is more evident by making explicit the dependence from the thermodynamic variables and the measured frequencies:

$$x_w(p, T) = \frac{\left[\frac{\epsilon_{\text{dry}}(p, T) \left(f_{\text{dry}} / f_{\text{mix}} \right)^2 - 1}{\epsilon_{\text{dry}}(p, T) \left(f_{\text{dry}} / f_{\text{mix}} \right)^2 + 2} \cdot \frac{\epsilon_{\text{dry}}(p, T) + 2}{\epsilon_{\text{dry}}(p, T) - 1} \right] - 1}{\rho_w(T) / \rho_{\text{dry}} - 1}, \quad (8)$$

which shows that any systematic error in the determination of p is cancelled out by the product of the inverted ratios in the numerator, because the multiplication by the squared frequency ratios has a negligible effect, their difference from unity being extremely small. As an example, for the fraction $x_w = 1000$ ppm of water in methane at 275 K and 150 kPa, $\left(f_{\text{dry}} / f_{\text{mix}} \right)^2 - 1 = 4.7 \times 10^{-6}$ and an error in the determination of the pressure of 150 Pa (relatively 0.1%) in the determination of p propagates through $\epsilon_{\text{dry}}(p, T)$ so that the numerator of Eq. (8) changes x_w by only 1 ppm. Thus, as the variability of p in the successive measurements of f_{dry} and f_{mix} is mainly determined by the precision of the pressure control (typically in the relative order of 1 part in 10^5), it has a negligible effect on x_w . The permittivity of the dry component $\epsilon_{\text{dry}}(p, T)$ may be either determined experimentally (from the squared ratios $\left(f_{\text{dry}} / f_0 \right)^2$ where f_0 are the vacuum microwave frequencies at the same temperature), or it can be calculated if some reliable assumption on the composition of the dry part is available *a priori*. In both cases, the determination of x_w from Eq. (8) turns out to be extremely robust against any systematic error in the measurement or evaluation of $\epsilon_{\text{dry}}(p, T)$.

Figure 8 illustrates a quantitative comparison of the overall uncertainty budget in a determination of x_w with the procedure described above and that used in Section 2, showing that a ten-fold reduction in the sensitivity to the uncertainty of pressure determinations is expected, with a consequent increase in the sensitivity of the microwave technique when x_w is low.

4 Microwave determination of the water fraction of a natural gas sample

1 The scheduled research activities of the Characterisation of Energy Gases (GAS) project [19] included in its
2 final stage (spring 2013) the validation of new methods, including microwave hygrometry, for comparing
3 humidity standards with humidity sensors used in industrial gas monitoring conditions. The location of such
4 tests was made available by courtesy of ENAGAS at their industrial facilities in Zaragoza (ES), where an
5 experimental rig suitable for measurements of humidity in natural gas samples was set-up thanks to a main
6 contribution of INTA. A comprehensive description of these tests, the variety of instruments and sensors
7 under test and the experimental results may be found in a separate paper submitted to this journal [7]. Here,
8 we focus on the outcome of the limited number of experiments which could be conducted using the
9 microwave apparatus within the limited time slot available for testing this method.

4.1 Preparation of the experiment for industrial tests

10 The apparatus briefly described in Section 2.1 underwent minor modifications to be adapted the industrial
11 measurement conditions and to reduce some critical deficiencies of its performance as evidenced in the
12 course of preliminary tests at INRiM. To enhance the sensitivity of the method for vapor phase
13 measurements of at low water fractions, and implement the procedure described above, a compact water
14 collection system was prepared. The system is based on the same design previously employed at NIST while
15 developing a gravimetric hygrometer [20] and is comprised by two hermetic stainless steel tubes with an
16 internal volume of 100 cm^3 which were respectively filled with anhydrous $\text{Mg}(\text{ClO}_4)_2$ and anhydrous P_2O_5 .
17 The valve configuration of the manifold incorporating these desiccant cartridges allows to alternatively
18 direct the gas flow through just one cartridge, or through both in series, or by-pass both. Use of magnesium
19 perchlorate, which is reported at explosion risk when in contact with a reducing atmosphere, was avoided
20 during tests with natural gas. A few other modifications to the scheme in Fig. 1 were brought to the
21 apparatus. These included the substitution of the mass-flow controller, not rated to work leak-proof above
22 800 kPa, with a manual flow regulating needle valve and the addition of a second such valve upstream the
23 PID controlled outlet electro-valve, in order to keep the pressure drop across it within the specifications. To
24 reduce thermal gradients within the microwave cavity, the pressure vessel containing the resonator was
25 inserted in a larger stainless steel container which was maintained evacuated in the course of the
26 measurements. Finally, the bulky and costly network analyzer which is ordinarily used to excite and detect
27 microwave resonances was substituted by a custom electronic instrument [21] which had been developed by

Politecnico di Torino within the course of the GAS project. The limited frequency range of this prototype (1 GHz to 6.9 GHz) allowed measurements with just one triply-degenerate cavity mode (TM11 at 5.14 GHz) preventing the microwave resonator to be used in condensation mode. To determine the frequencies and half-widths of the TM11 triplet, the prototype was set to sweep through 201 frequencies, spanning approximately 16 MHz and centered approximately at the average triplet frequency. The complex voltage data returned by the prototype for the scattering parameter S_{21} were fitted with a standard function [21]. The typical precision of the fit allowed to determine the frequency and halfwidth of TM11 mode with a relative uncertainty of 50 ppb.

4.2 Experimental test of a natural gas sample with variable humidity

A demanding preparative work, which included assembling the gas manifold, instrumentation and sensors and their electrical connections, followed by careful helium leak testing of the complete experimental rig, which included several prototype instruments and commercial sensors, severely limited the time slot available for experimental testing with the microwave method. Also, the particular specifications or features of some of the instrumentation on the rig, initially limited the maximum working pressure at 750 kPa. At this moderate pressure, the extreme dryness of the natural gas sample made available by ENAGAS, with an estimated water fraction of only 4 ppm, from measurements performed using a diode laser adsorption spectrometer, and a resulting hydrocarbon dew point higher than the water dew point, are extremely challenging for several techniques (including microwave hygrometry) and discouraged from attempting to achieve accurate humidity measurements of the sample in its original condition. For the purpose of varying the humidity content of natural gas a custom built high-pressure divided flow humidity generator prepared by INTA was available [7]. For an initial test the generator was regulated until a nominal reference humidity as recorded by a polymer sensor and an Al_2O_3 operating at the same pressure as the microwave hygrometer provided a stable reading corresponding to a water fraction of approximately 150 ppm. By then, the gas was admitted to flow through the microwave resonator at a rate of about 1000 sccm while the temperature and pressure of the cavity were maintained stable by suitable PID controls at (297.00 ± 0.01) K, (752.00 ± 0.01) kPa. Microwave data for the TM11 mode were then repeatedly recorded using the prototype electronic instrumentation at the rate of one acquisition every 70 s for a total time lapse of 75 mins and stored in a portable PC for successive analysis. Following this initial acquisition, we diverted the flow within the water collection manifold upstream the microwave apparatus, through the P_2O_5 cartridge, to implement the drying process for the measurement procedure described in Section 4. This change caused a relative increase of the

TM11 frequency by approximately 6000 ppm which needed approximately 30 mins to be completed.

Additional recording of dry gas microwave data was then continued for 15 mins and these results were later averaged providing an estimate the reference frequency f_{dry} needed in Eq. 4 and Eq. 8 to calculate the permittivity of the mixture and hence the water fraction. The drying manifold was then by-passed returning to the initial condition (nominal water fraction of 150 ppm) to check repeatability, and TM11 data were recorded for an other hour. Finally, the humidity generator was set to reduce the nominal water fraction from 150 ppm to about 65 ppm and microwave data were acquired for a further 30 mins.

The temporal evolution of the TM11 frequency during the separate phases of this test is displayed in Fig. 9. In the initial phase of the test, when x_w is maintained constant at the nominal value of 175 ppm, some instability of the measured microwave signal is evident. Also, after the gas flow by-passes the dryer for the second time, the repeatability of the microwave signal for nearly the same (160 ppm) nominal composition is not satisfactory. The originating cause of this limited performance is not currently known, though it is likely to be related to changes of the gas flow-rate, which was not controlled and only roughly measured with a variable area flowmeter during the test. Variations of the flow-rate might have induced temporary changes of the density of the gas which were not revealed by temperature and pressure measurements on the resonator and its containing vessel.

Over the course of the entire experimental test, for the sake of comparison with the microwave estimate of x_w , humidity data were continuously acquired by several commercial instruments from different manufacturers [7], including several capacitive metal oxide sorbtive sensors (Al_2O_3 , P_2O_5), as well as a diode laser absorption spectrometer and polymer sensors. All these instruments were installed in series/parallel branches upstream the microwave apparatus, receiving the same gas flow from the humidity generator. Finally, detailed and accurate chromatographic analysis of the natural gas sample was continuously recorded by the ENAGAS central laboratory, providing information on the hydrocarbon fractions (up to C_{12}) and other constituents the dry part of the mixture. The results of such analysis for the present test are reported in Table II.

4.3 Analysis of microwave results

To obtain microwave estimates of x_w we use the procedure described by Eqs. (4) to (8) in Section 4, where the quantity f_{mix} corresponds to the fitted mean frequency of mode TM11 at each successive data acquisition and the quantity $f_{\text{dry}} = (5138.4790 \pm 0.0005)$ MHz is the average of about 20 successive measurements recorded after the frequency increase caused by distracting the gas flow through the P_2O_5

drier had completed and stabilized. We remark that the frequency perturbations of the QSR due to skin effect, cavity shape, and the presence of ducts and waveguides all have a negligible effect on the calculated value of ε_{mix} from the squared ratios in Eq. 4 as far as the temperature and pressure remain approximately constant during the alternative measurements with the humid and the dry mixture. These perturbation corrections, as well as other small adjustments to account for slight differences of the experimental temperature and pressure of each single datum, can safely be ignored in this context.

In order to use Eq. 4 and Eq. 7 for the calculation of x_w , estimates of permittivity ε_{dry} and the polarizability ρ_{dry} (i.e. the density) of the dry part of the mixture are needed. Fortunately, these estimates do not need to be accurate and can be provided using different approaches. Firstly, by conjecturing the composition of the dry part, with a guess supported by more or less reliable independent information. Thus, for the present case we could either simply assume that the dry constituent of the mixture is pure methane or we may use the more detailed composition analysis in Table II. If the latter is chosen, both the dielectric constant and the density are available as interpolated functions of p and T from accurate literature sources. Alternatively, we may determine ε_{dry} from our recorded dry frequency data f_{dry} and a previous interpolation of the vacuum frequencies of the cavity $f_0(T)$ using Eq. 1. It is remarkable that, independently from the particular choice among these alternatives, the relative variation of the calculated molar fraction x_w in the course of the experiment described in the previous section is always less than 1 ppm. In fact the squared frequency ratio $(f_{\text{dry}}/f_0)^2$ determines $\varepsilon_{\text{dry}} = 1.006\,478$ in remarkable agreement with $\varepsilon_{\text{dry}}^{\text{REF}} = 1.006\,472$ independently estimated using the data in Table II and [10]. Figure 9 displays the microwave determination of x_w , which is found to be consistent within the large dispersion of the recorded readings from the entire set of commercial humidity sensors.

5 Conclusions and future perspectives

The preliminary tests described in this work demonstrate that microwave measurements are capable of achieving measurements with a useful uncertainty and sensitivity for natural gas hygrometry. However, the tests reported have only partially explored the potential of this technique. Future investigation should move along the lines of exploring a wider temperature and pressure range with a smaller, faster time responding instrument. Speculating about the salient features of such instrument, to enhance sensitivity and accuracy it should be capable of a more direct comparison of the permittivity of the humid and dried parts of the sample under test while minimizing possible variations of the density in the course of the comparison. These requisites may be satisfied by a compact double microwave cavity with reduced dimensions and mass which

would enhance temperature uniformity and minimize time response. Separate flow of the humid and dry gases would be directed through the two cavities while these would be subject to a single flow and pressure control. Finally, working in condensation mode, it would be worth investigating if the microwave cavity could be sensitive and useful in those cases when co-condensation of heavier hydrocarbons and water takes place.

Acknowledgments

This reported activity was carried out in the frame of the Joint Research Project “ENG01, Characterisation of Energy Gases (GAS)” running under the European Metrology Research Program.

References

- 1 1. S. Bell, R. Benyon, N. Böse, M. Heinonen, *Int. J. Thermophys.* **29**, 1537 (2008)
- 2 2. E. F. May, R. C. Miller, *J. Chem. Eng. Data* **47**, 102 (2002)
- 3 3. E. F. May, T. J. Edwards, A. G. Mann, C. Edwards, *Int. J. Thermophys.* **24**, 1509 (2003)
- 4 4. A. R. H. Goodwin, J. B. Mehl, M. R. Moldover, *Rev. Sci. Instrum.* **67**, 4294 (1996)
- 5 5. R. Cuccaro, R. M. Gavioso, G. Benedetto, D. Madonna Ripa, V. Fericola, C. Guianvarc'h *Int. J. Thermophys.* **33** 1352 (2011)
- 6 6. R. J. Underwood, R. Cuccaro, S. Bell, R. M. Gavioso, M. Stevens, M. de Podesta *Meas. Sci. Tech.* **23**, 085905 (2012).
- 7 7. R. Benyon, J. G. Gallegos, S. Avila, A. Benito, H. Mitter, S. Bell, M. Stevens, N. Böse, V. Ebert, M. Heinonen, H. Sairanen, A. Peruzzi, R. M. Gavioso, M. Val'ková, An investigation of the comparative performance of diverse humidity sensing techniques in natural gas, submitted to *Int. J. Thermophys.* (2013)
- 8 8. R. Span, E.W. Lemmon, R.T. Jacobsen, W. Wagner, A. Yokozeki, *J. Phys. Chem. Ref. Data* **29**, 1361 (2000).
- 9 9. U. Setzmann, W. Wagner, *J. Phys. Chem. Ref. Data* **20**, 1061 (1991)
- 10 10. J. W. Schmidt, M. R. Moldover *Int. J. Thermophys.* **24**, 375 (2003)
- 11 11. W. Wagner, A. Pruß, *J. Phys. Chem. Ref. Data* **31**, 387 (2002).
- 12 12. O. Akin-Ojo, A. H. Harvey, K. Szalewicz, *J. Chem. Phys.* **125**, 014314 (2006).
- 13 13. G. Birnbaum, S.K. Chatterjee, *J. Appl. Phys.* **23**, 220 (1952).
- 14 14. A.H. Harvey, E.W. Lemmon, *Int. J. Thermophys.* **26**, 31 (2005).
- 15 15. V. A. Rabinovich, V. G. Beketov, *Moist Gases: Thermodynamic Properties*, (Begell House, New York, 1995).
- 16 16. M. Heinonen (private communication)
- 17 17. K. Fattah, *A Prediction of Water content in Sour Natural Gas*, Research Report no. 28/426, College of Engineering, King Saud University (2007).
- 18 18. R. F. Bukacek, *Equilibrium Moisture Content of Natural Gases*, Research Bulletin 8, Institute of Gas Technology, 1955).
- 19 19. http://www.euramet.org/fileadmin/docs/EMRP/JRP/JRP_Summaries_2009/ENG01_Publishable_JRP_Summary.pdf

20. C. W. Meyer, J. T. Hodges, R. W. Hyland, G. E. Scace, J. Valencia-Rodriguez, J R Whetstone,
Metrologia **47**, 192 (2010)

21. S. Corbellini, R. M. Gavioso, IEEE Trans. Instr. Meas. **62**, 1259 (2013)

1
2
3
4
5
6
7
8
9
10
11
12
13
14
15
16
17
18
19
20
21
22
23
24
25
26
27
28
29
30
31
32
33
34
35
36
37
38
39
40
41
42
43
44
45
46
47
48
49
50
51
52
53
54
55
56
57
58
59
60
61
62
63
64
65

Table 1 Repeatability of the TM11/TE11 ratio in different measurement conditions

Fluid	Measurement conditions	TM11/TE11 ratio mean value	TM11/TE11 ratio standard dev.
vacuum	300 K ÷ 350 K	0.610 598 015	0.000 000 071
dry N ₂	294 K, 200 kPa ÷ 1.5 MPa	0.610 598 009	0.000 000 032
dry CH ₄	293 K, 150 kPa ÷ 1.0 MPa	0.610 598 008	0.000 000 011
CH ₄ +H ₂ O	293 K, 150 kPa ÷ 1.0 MPa	0.610 598 007	0.000 000 084

1
2
3
4
5
6
7
8
9
10
11
12
13
14
15
16
17
18
19
20
21
22
23
24
25
26
27
28
29
30
31
32
33
34
35
36
37
38
39
40
41
42
43
44
45
46
47
48
49
50
51
52
53
54
55
56
57
58
59
60
61
62
63
64
65

Table 2 Gas chromatographic ENAGAS analysis of the composition of a natural gas sample

Component	Molar Fraction and uncertainty ^a (%)
Methane	90.43 ± 0.12
Ethane	6.46 ± 0.09
Propane	1.32 ± 0.02
Nitrogen	0.90 ± 0.03
Carbon dioxide	0.30 ± 0.01
i-Butane	0.210 ± 0.007
n-Butane	0.275 ± 0.007
i-Pentane	0.037 ± 0.001
n-Pentane	0.031 ± 0.001
C ₆ +	< 0.04

^a expanded uncertainties with coverage factor $k = 2$

Figure Captions

1 **Fig. 1** Schematic diagram of the gas manifold used for microwave measurements in humid methane and
2 natural gas. The humidity generator used for methane measurements at INRiM was maintained at
3 273.15 K by a water-ice bath. For natural gas measurements the humidity generator was working at
4 ambient temperature. The chemical dryer was used only for natural gas measurements.
5

6 **Fig. 2** Fractional deviations (ppm) between experimental determinations of the dielectric constant of N₂
7 (left) and CH₄ (right) and their calculated values. The arrows reconstruct the temporal sequence of
8 the measurements: N₂ - increasing p from 500 kPa up to 1.5 MPa and decreasing from 1.5 MPa to
9 200 kPa; CH₄ - increasing p from 300 kPa up to 1.0 MPa and decreasing from 1.0 MPa to 150 kPa.
10
11

12 **Fig. 3** Water volume fraction x_w generated by the coarse saturator at (4.0 ± 0.5) °C determined from
13 microwave measurements in the QSR - Left: temporal oscillations of x_w (red dots) evidence the
14 imperfect thermostating of the saturator at low pressure (blue dashed line) – Right: x_w plotted as a
15 function of pressure; the blue line is the function $x_{eq} = e_w(T_{Sat})/p$ with $T_{Sat} \approx 4$ °C.
16
17

18 **Fig. 4** Relative variation (in ppb) of TM11/TE11 frequency ratios from their mean reference value during
19 measurements in dry CH₄ at different pressures. The scatter of the plotted data display the precision
20 of repeated frequency measurements.
21
22
23

24 **Fig. 5** (Top) Condensation test for humid methane at 150 kPa. The dew-point of the mixture (blue line) is
25 determined by maintaining a constant relative difference (-2000 ppb) of the measured ratio
26 TM11/TE11 (red line) from its reference value. This choice corresponds to maintaining a volume
27 of 1.2 mm^3 of condensed water on the resonator surface, with an average layer thickness of 150
28 nm. (Bottom) Condensation test for humid methane at 750 kPa.
29
30

31 **Fig. 6** Enhancement factor f of a humid methane mixture at 273.25 K at 150 kPa and 750 kPa. Red lines
32 and shaded area delimit the overall uncertainty $u(f)$ estimated considering the contributions of
33 imperfect temperature and pressure measurements and the discrepancy between the experimental
34 and calculated permittivity of dry methane.
35
36

37 **Fig. 7** Comparison of the experimental determination of the enhancement factor of humid methane
38 determined in this work with data adapted from correlations of water content in natural gas. The red
39 lines and the grey shaded area delimit the overall dispersion of literature data [16 - 18].
40
41
42

43 **Fig. 8** Comparison of the relative overall uncertainties achievable in the determination of the molar
44 fraction x_w of a humid methane mixture at 293 K, 100 kPa with two different methods: (red) direct
45 procedure described in Section 2 and Ref. 5; (blue) relative procedure described in Section 4. The
46 uncertainty budget includes contributions $u(p)=100$ Pa and $u(T)=0.01$ K from pressure and
47 temperature measurements, and from reference functions or correlations predicting the
48 thermodynamic and electrical properties of methane and water.
49
50
51

52 **Fig. 9** Microwave determination of the water fraction of a natural gas sample of variable humidity. Top:
53 relative frequency change recorded for mode TM11 during the different phases of the test; x_w^{ref} is
54 the nominal water fraction recorded by a calibrated Al₂O₃ sensor. Bottom: comparison of the
55 microwave estimate of x_w (blue curve) with the recorded readings of several commercial
56 instruments and humidity sensors.
57
58
59
60
61
62
63
64
65

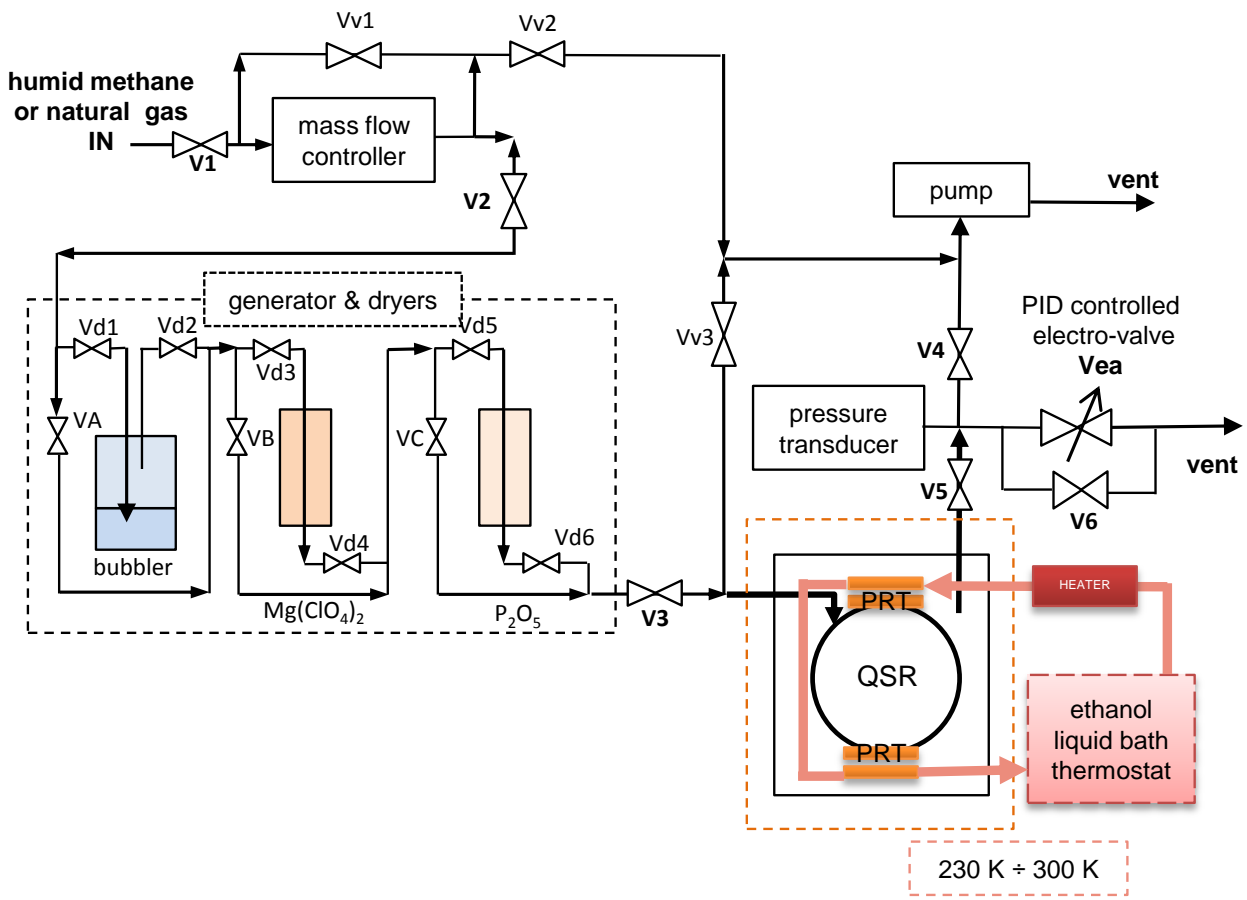


Fig. 1

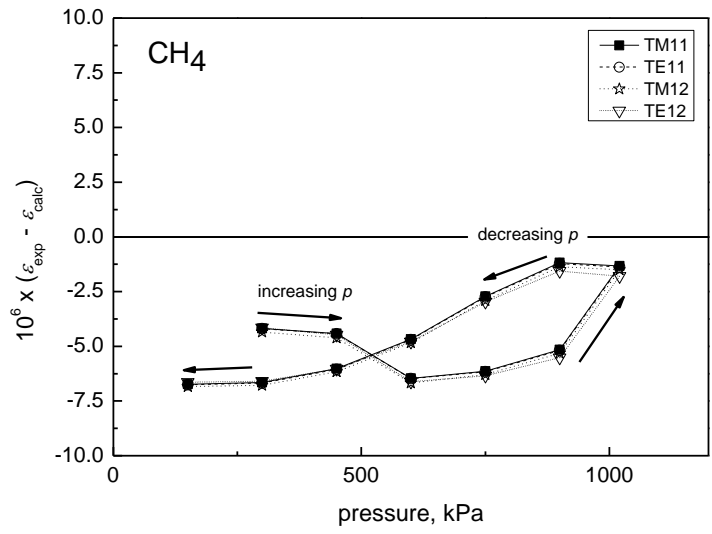
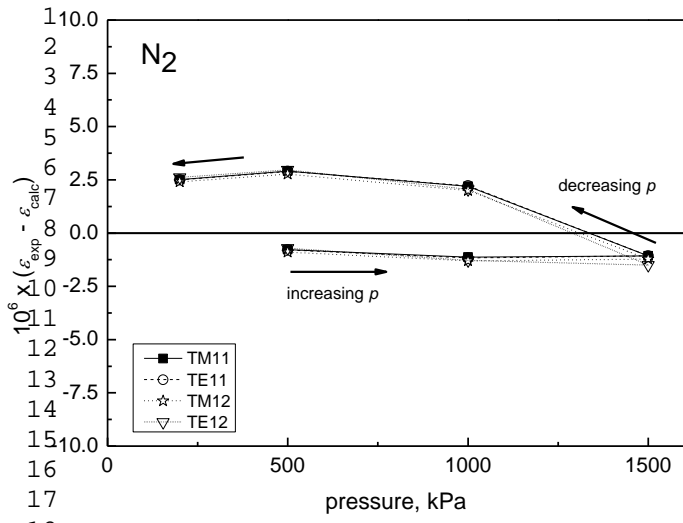


Fig. 2

1
2
3
4
5
6
7
8
9
10
11
12
13
14
15
16
17
18
19
20
21
22
23
24
25
26
27
28
29
30
31
32
33
34
35
36
37
38
39
40
41
42
43
44
45
46
47
48
49
50
51
52
53
54
55
56
57
58
59
60
61
62
63
64
65

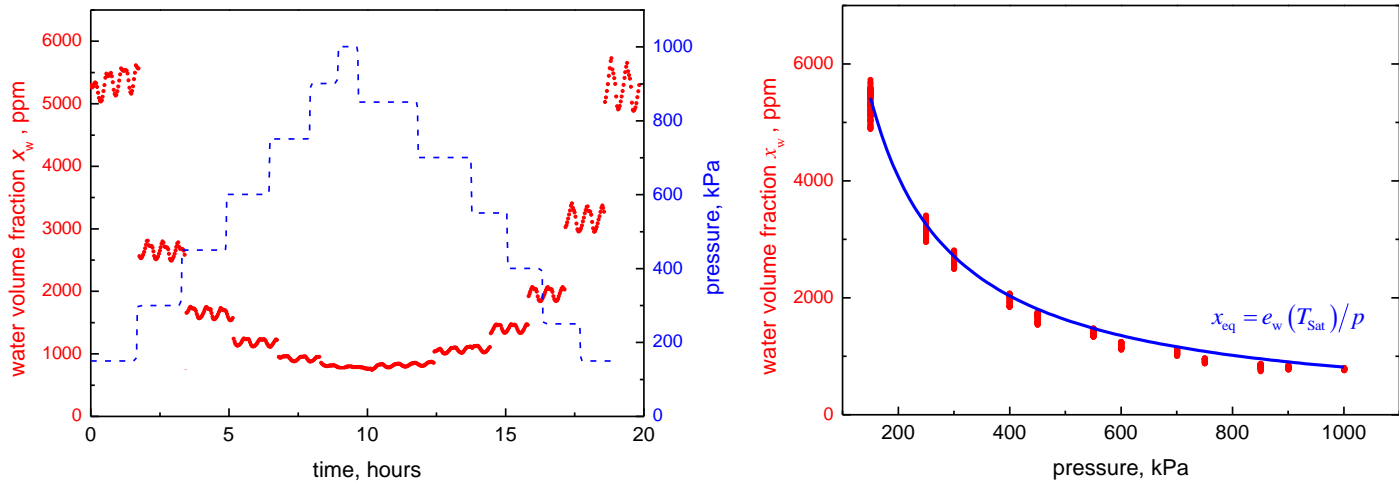


Fig. 3

1
2
3
4
5
6
7
8
9
10
11
12
13
14
15
16
17
18
19
20
21
22
23
24
25
26
27
28
29
30
31
32
33
34
35
36
37
38
39
40
41
42
43
44
45
46
47
48
49
50
51
52
53
54
55
56
57
58
59
60
61
62
63
64
65

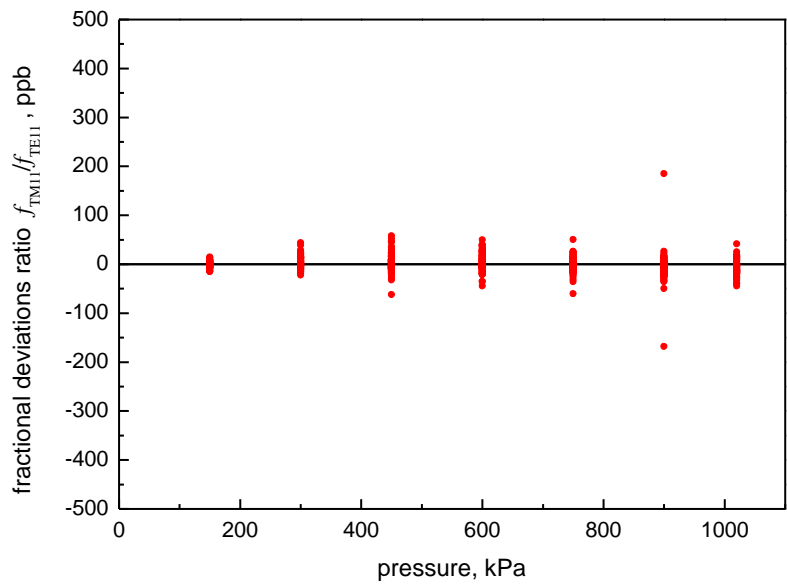


Fig. 4

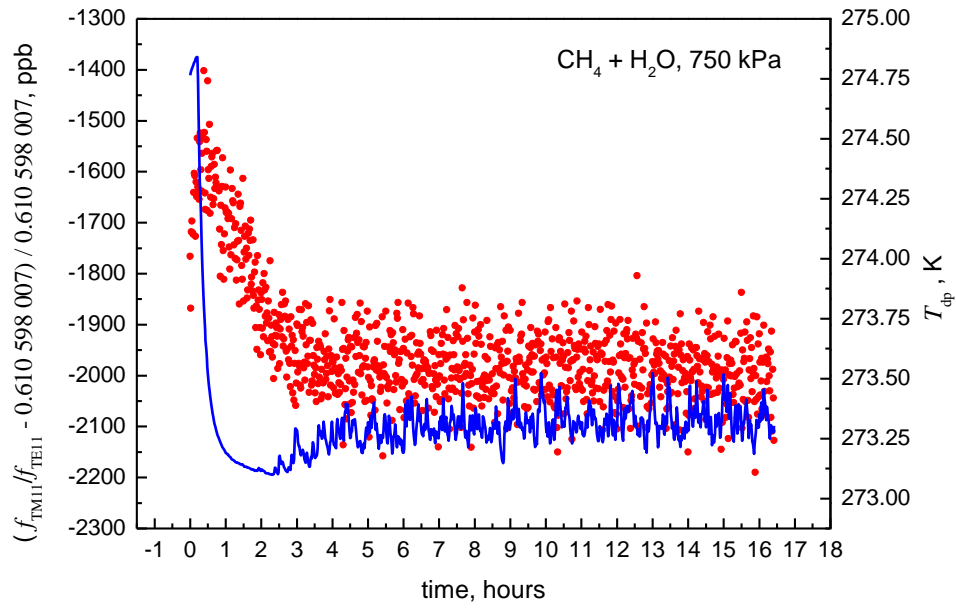
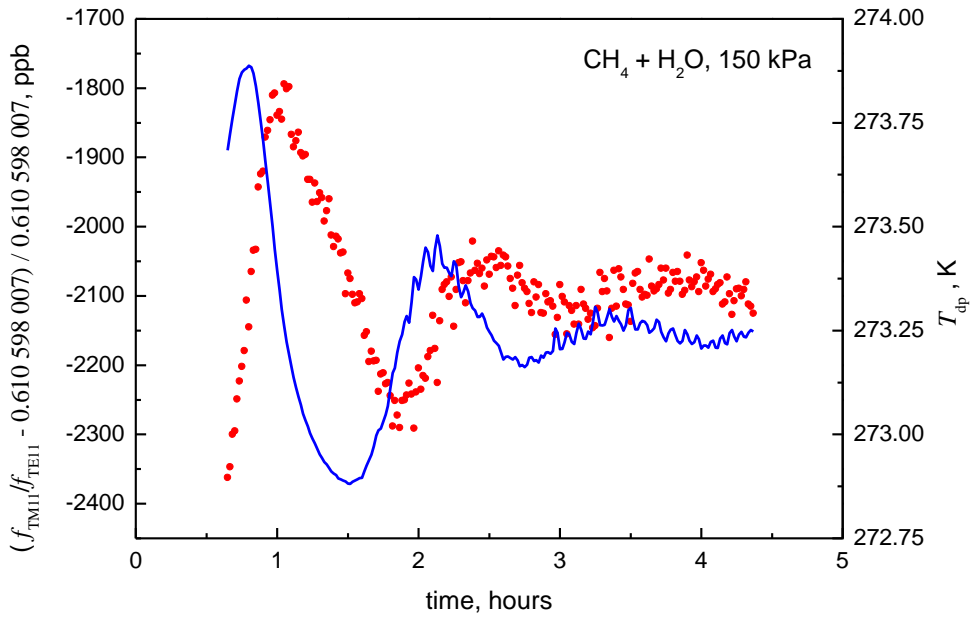


Fig. 5

1
2
3
4
5
6
7
8
9
10
11
12
13
14
15
16
17
18
19
20
21
22
23
24
25
26
27
28
29
30
31
32
33
34
35
36
37
38
39
40
41
42
43
44
45
46
47
48
49
50
51
52
53
54
55
56
57
58
59
60
61
62
63
64
65

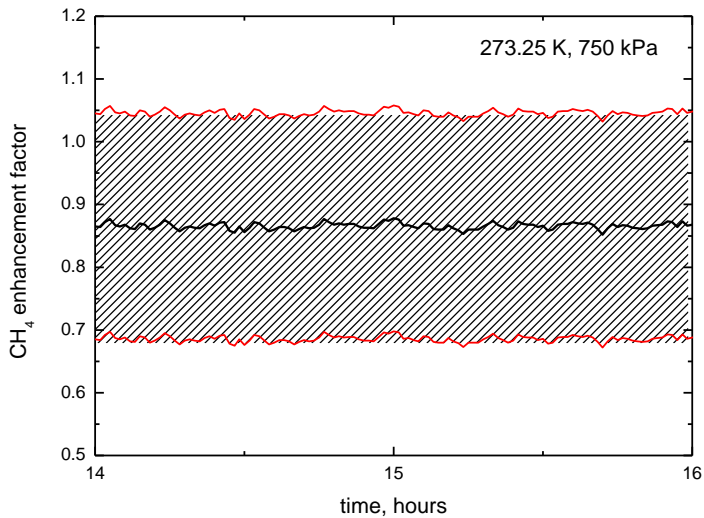
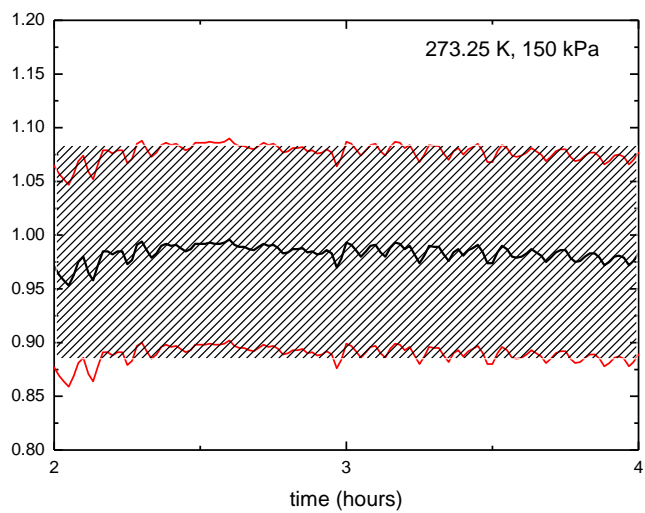


Fig. 6

1
2
3
4
5
6
7
8
9
10
11
12
13
14
15
16
17
18
19
20
21
22
23
24
25
26
27
28
29
30
31
32
33
34
35
36
37
38
39
40
41
42
43
44
45
46
47
48
49
50
51
52
53
54
55
56
57
58
59
60
61
62
63
64
65

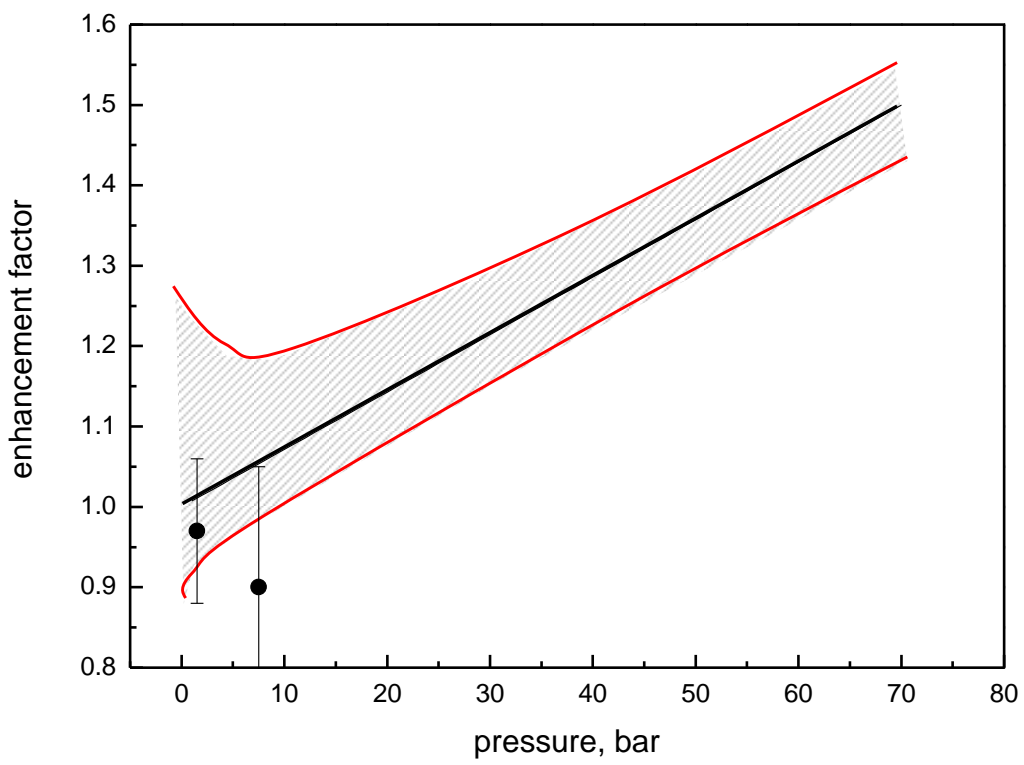


Fig. 7

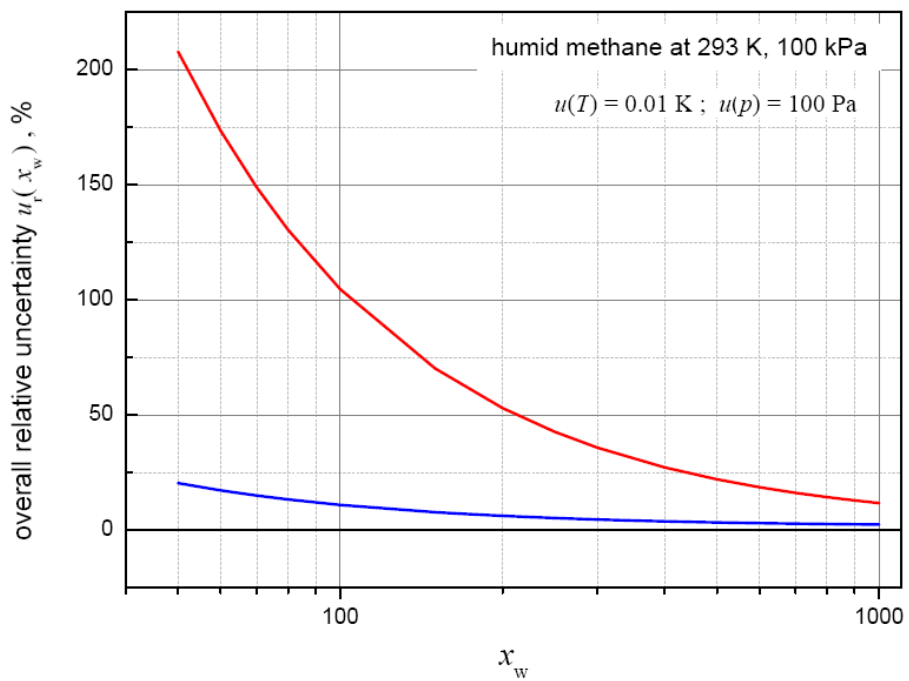


Fig. 8

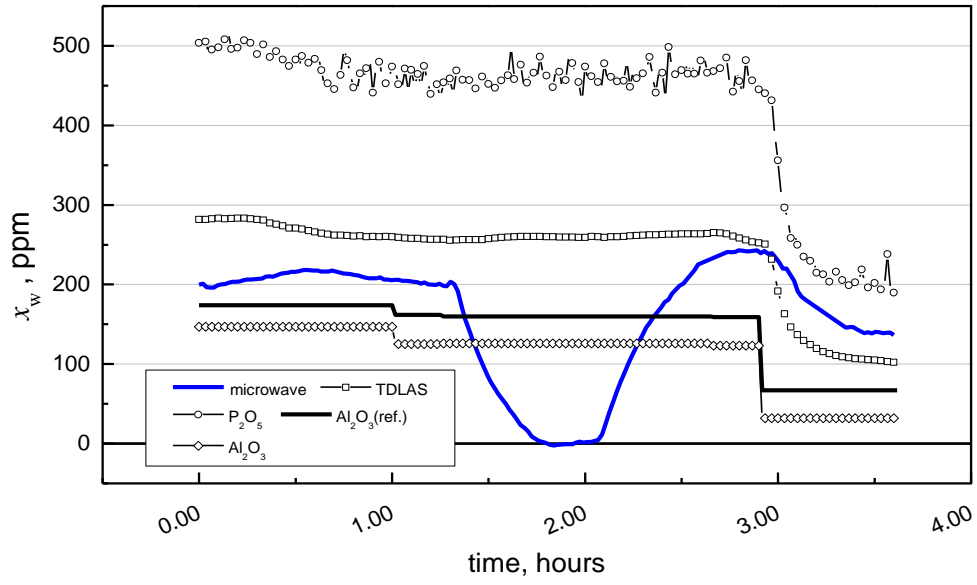
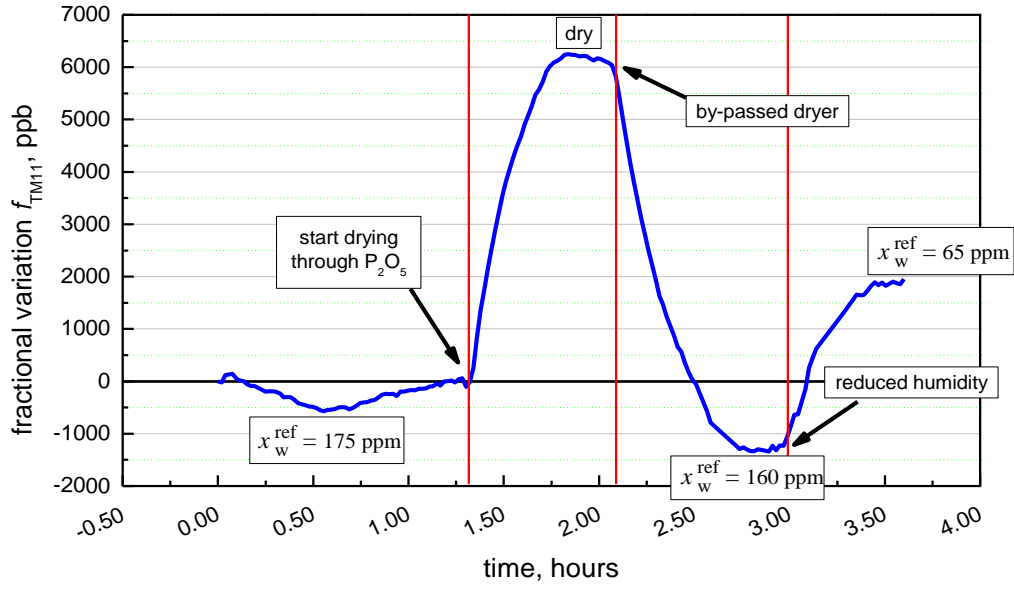


Fig. 9